The primary cilium coordinates early cardiogenesis and hedgehog signaling in cardiomyocyte differentiation

Christian A. Clement[1], Stine G. Kristensen[1], Kjeld Møllgård[2], Gregory J. Pazour[3], Bradley K. Yoder[4], Lars A. Larsen[5] and Søren T. Christensen[1,*]

[1]Department of Biology, University of Copenhagen, Universitetsparken 13, DK-2100 Copenhagen, Denmark
[2]Department of Cellular and Molecular Medicine and [5]Wilhelm Johannsen Centre for Functional Genome Research, University of Copenhagen, Blegdamsvej 3, DK-2200 Copenhagen, Denmark
[3]University of Massachusetts Medical School Worcester, Worcester, MA 01655, USA
[4]The University of Alabama at Birmingham, Birmingham, AL 35294, USA
*Author for correspondence (stchristensen@bio.ku.dk)

Accepted 29 May 2009
Journal of Cell Science 122, 3070-3082 Published by The Company of Biologists 2009
doi:10.1242/jcs.049676

Summary

Defects in the assembly or function of primary cilia, which are sensory organelles, are tightly coupled to developmental defects and diseases in mammals. Here, we investigated the function of the primary cilium in regulating hedgehog signaling and early cardiogenesis. We report that the pluripotent P19.CL6 mouse stem cell line, which can differentiate into beating cardiomyocytes, forms primary cilia that contain essential components of the hedgehog pathway, including Smoothened, Patched-1 and Gli2. Knockdown of the primary cilium by Ift88 and Ift20 siRNA or treatment with cyclopamine, an inhibitor of Smoothened, blocks hedgehog signaling in P19.CL6 cells, as well as differentiation of the cells into beating cardiomyocytes. E11.5 embryos of the *Ift88*^{tm1Rpw} (Ift88-null) mice, which form no cilia, have ventricular dilation, decreased myocardial trabeculation and abnormal outflow tract development. These data support the conclusion that cardiac primary cilia are crucial in early heart development, where they partly coordinate hedgehog signaling.

Supplementary material available online at
http://jcs.biologists.org/cgi/content/full/122/17/3070/DC1

Key words: Primary cilia, P19.CL6 cells, Cardiac development, Mouse, Heart, Hedgehog signaling, siRNA, Ift88, Ift20, Cyclopamine

Introduction

Heart development in vertebrates is initiated in embryos shortly after gastrulation by aggregation of cardiomyocyte progenitor cells that become allocated from the mesodermal population (Sucov, 1998). The mouse embryonal carcinoma (EC) P19 cell line is a common cell model system to study early heart differentiation in vitro because the P19 EC cells can differentiate into beating cardiomyocytes when stimulated with dimethyl sulfoxide (DMSO) (Skerjanc, 1999; Paquin et al., 2002). The heart transcription factors Gata4 and Nkx2-5 are markers for early cardiomyocyte differentiation (Grépin et al., 1997; Lints et al., 1993). Gata4 is a tissue-restricted transcription factor that is found in the heart but not in skeletal muscle (Grépin et al., 1994) and is necessary for proper heart tube development at the ventral midline (Kuo et al., 1997). The *Gata4* and *Nkx2-5* genes are, together with MEF2C, desmin and cardiac actin, expressed in the cardiomyocyte population before fusion of the linear heart tube (Lyons, 1994). Mice lacking Gata4 and Nkx2-5 die because of severe defects in heart formation (Sucov, 1998).

A series of signal transduction systems have been implicated as essential coordinators of early cardiogenesis, including hedgehog (Hh), Wnt, bone morphogenetic protein (BMP) and platelet-derived growth factor receptor (PDGFR) signaling (Washington Smoak et al., 2005; Kwon et al., 2008; Hirata et al., 2007; van Wijk et al., 2007). In mammals, Hh signaling is induced by three different ligands, including Sonic hedgehog (Shh), which controls left-right asymmetry, digit patterning in the limbs and development of the lung and heart (Tsukui et al., 1999; Johnson et al., 1994; Bellusci et al., 1997; Washington Smoak et al., 2005). In the adult mouse heart, Hh signaling is required for proangiogenic gene expression and maintenance of the adult coronary vasculature, and it specifically controls the survival of small coronary arteries and capillaries (Lavine et al., 2008). In vertebrates, the secreted Hh proteins bind to the transmembrane patched protein-1 (Ptc1) hereby abolishing the inhibitory effect of Ptc1 on the seven-transmembrane receptor Smoothened (Smo). This allows Smo to transduce a signal via Gli transcription factors to the nucleus for expression of Hh target genes. There are three Gli transcription factors, Gli1-Gli3. Gli1 functions as a constitutive activator (Hynes et al., 1997; Ruiz I Altaba, 1999), whereas Gli2 and Gli3 have an N-terminal transcriptional repressor domain and a C-terminal transcription activator domain. Smo might be the controlling molecule in the Hh signaling pathway that mediates the proteolytic events between the activating and repressing form of Gli2 and Gli3 in an Hh-dependent manner (Huangfu and Anderson, 2006). P19 EC cells normally require aggregation to form embryoid bodies in suspension induced by DMSO before differentiation analysis (Skerjanc, 1999). However, overexpression of Shh has been observed to induce the expression of cardiac muscle factors Gata4 and Nkx2-5 via Gli1and Gli2, which results in differentiation of the cells into cardiomyocytes in the absence of DMSO (Gianakopoulos and Skerjanc, 2005). This supports the conclusion that Hh signaling is critical during early

cardiogenesis. Therefore, P19 EC cells offer a unique model cell system to investigate the mechanisms by which Hh signaling is coordinated by the cells during differentiation in early cardiogenesis.

Recent reports have indicated that primary cilia have an important role in an array of vertebrate developmental processes. Primary cilia are microtubule-based organelles, organized in a 9+0 axonemal ultrastructure, which are assembled and maintained via a process termed intraflagellar transport (IFT) in most mammalian cells during growth arrest (Rosenbaum and Witman, 2002; Pedersen et al., 2008). Primary cilia are thought to function as mechano- and chemosensory organelles that specifically coordinate a series of cellular signal transduction pathways during development and in tissue homeostasis, including Hedgehog (Hh), PDGFRα and Wnt signaling (reviewed by Christensen et al., 2007; Christensen et al., 2008; Wong and Reiter, 2008; Gerdes and Katsanis, 2008). Consequently, defects in assembly of the primary cilium or mutations in ciliary signaling components lead to severe developmental diseases and disorders, now referred to as ciliopathies (reviewed by Pan, 2008; Lehmann et al., 2008; Davenport and Yoder, 2005). One of the first diseases to be related to dysfunctional primary cilia, was polycystic kidney disease (PKD), which was originally identified in mice mutated in the gene encoding Ift88/Polaris in the Oak Ridge Polycystic Kidney mouse (ORPK mouse, *Ift88*^{orpk} or *Ift88*^{Tg737NRpw}) (Moyer et al., 1994). Ift88 is a subunit of the IFT particle complex B required for functional IFT and assembly of the primary cilium (Pazour et al., 2000; Murcia et al., 2000; Haycraft et al., 2001; Taulman et al., 2001; Yoder et al., 2002; Lucker et al., 2005). No other function of Ift88 is known, and genes encoding IFT are found only in organisms that possess cilia.

Many of the essential Hh signaling components, such as Gli2, Gli3, Smo and Ptc, localize to primary cilia in a number of cell types, including fibroblasts (Haycraft et al., 2005; Rohatgi et al., 2007), epithelial cells in renal tubules (Harris and Torres, 2009) and the exocrine duct of the pancreas (Nielsen et al., 2008), as well as in human embryonic stem cells (Kiprilov et al., 2008; Breunig et al., 2008). It was suggested that the concerted movement of Smo and Ptc into and out of the cilium creates a switch by which cells can turn Hh signaling on and off during development and tissue homeostasis (Corbit et al., 2005; Rohatgi et al., 2007; Christensen and Ott, 2007). In this scenario, binding of ligands to Ptc in the cilium might activate the Hh pathway by removal of Ptc from the cilium in a process that is associated with ciliary enrichment of Smo (Rohatgi et al., 2007). In vitro activation of Smo in cells exposed to Shh is blocked in mouse embryonic fibroblasts (MEFs) lacking Ift172 or the dynein retrograde motor, Dync2h1 (Ocbina and Anderson, 2008). The heterotrimeric kinesin complex comprising the motor subunits Kif3a and Kif3b and the nonmotor protein KAP is responsible for microtubule-based anterograde translocation destined for membranous organelles, as well as for ciliogenesis (Yamazaki et al., 1995; Haraquchi et al., 2006).

Furthermore, in mice lacking Kif3a and Smo there is a failure in the maturation of radial astrocytes that would normally develop into the dentate gyrus, which is responsible for maintenance of adult neurogenesis (Han et al., 2008). Disruption of Kif3a results in severe developmental abnormalities in the neural tube, cardiovascular insufficiencies and randomized left-right development (Takeda et al., 1999; Nonaka et al., 1998). Consequently, mutations in IFT proteins and other proteins associated with the cilium and the centrosome might result in dysfunctional Hh signaling and/or Gli processing with severe developmental disorders in mammals, including skeletogenesis (Gouttenoire et al., 2007), limb development (Haycraft et al., 2007), neural tube formation (Gorivodsky et al., 2008), cerebellar development (Chizhikov et al., 2007; Spassky et al., 2008), mammary gland development and defects in ovarian function (Johnson et al., 2008). Recently, Brueckner and co-workers (Slough et al., 2008) showed that the embryo heart at embryonic day 9.5 (E9.5) in *Kif3a*$^{-/-}$ mice has abnormal development of endocardial cushions (ECCs) and reduced trabeculation, indicating that primary cilium could coordinate processes in cardiac morphogenesis.

Since Kif3 family proteins regulate cellular processes in mammalian cells that are not necessarily related to the primary cilium (Teng et al., 2005; Haraguchi et al., 2006; Corbit et al., 2008), there is a need for a more thorough investigation on the role of the primary cilium in early cardiogenesis and Hh signaling, which is crucial for cardiomyocyte differentiation. In this study, we investigated the role of the primary cilium in Hh signaling and early cardiogenesis by: (1) characterization of primary cilia and their role in Hh signaling and differentiation of the pluripotent P19.CL6 cell line, an isolated subclone from the P19 cell line, into cardiomyocytes and (2) microscopy analysis of defects in heart development in E11.5 embryos from wild-type (WT) and Ift88-null (*Ift88*^{tm1Rpw}) mice. P19.CL6 cells have no requirement for being cultured in suspension and form embryoid bodies before differentiation (Uchida et al., 2007). This allowed us to follow the function of the primary cilium in the initial phases of differentiation from day 1 over a 2 week period, until beating cardiomyocytes formed. By analyzing the protein and mRNA levels of Gata4, Nkx2-5 and α-actinin, we can determine the effect on cardiogenesis when shutting down Hh signaling with cyclopamine treatment, a Smo-specific antagonist (Chen et al., 2002), or knocking down primary cilia by Ift88 and Ift20 siRNA. Ift20 is associated with the Golgi complex, and knockdown of this IFT particle reduces ciliary assembly without affecting Golgi structure (Follit et al., 2006). We show here that P19.CL6 cells form primary cilia and that Hh signaling components such as Ptc1, Smo and Gli2 localize to the cilia in these cells. Furthermore, cyclopamine halts Hh signaling, preventing P19.CL6 cells from forming beating clusters of cardiomyocytes. Ift88 and Ift20 siRNA nucleofection strongly reduced the assembly of primary cilia, mRNA and protein levels of Gata4, Nkx2-5 and α-actinin, expression of Ptc1 and Gli1, and nuclear localization of Gli1. Furthermore, the induced loss of primary cilia with Ift88 and Ift20 siRNA reduced and delayed the number of beating clusters of cardiomyocytes. In E11.5 embryos of Ift88-null (*Ift88*$^{-/-}$) mice, which lack primary cilia, we saw ventricular dilation, abnormal outflow tract development and abnormal myocardial trabeculae morphology compared with the wild type. These data support the conclusion that primary cilia are crucial for differentiation of P19.CL6 cells into cardiomyocytes and in early heart development in the mouse, partly via coordination of Hh signaling.

Results

P19.CL6 cell morphology and the effect of cyclopamine on cardiomyocyte differentiation

To investigate the cellular events during early heart development, we studied the morphology and changes in expression of cardiac transcription factors in P19.CL6 cell cultures during their differentiation into cardiomyocytes over a 2 week period. We first analyzed the effect of cyclopamine on Hh signaling and cardiomyogenesis (Fig. 1). Addition of 1% DMSO to the growth medium of P19.CL6 cells led to the formation of 15-20 beating

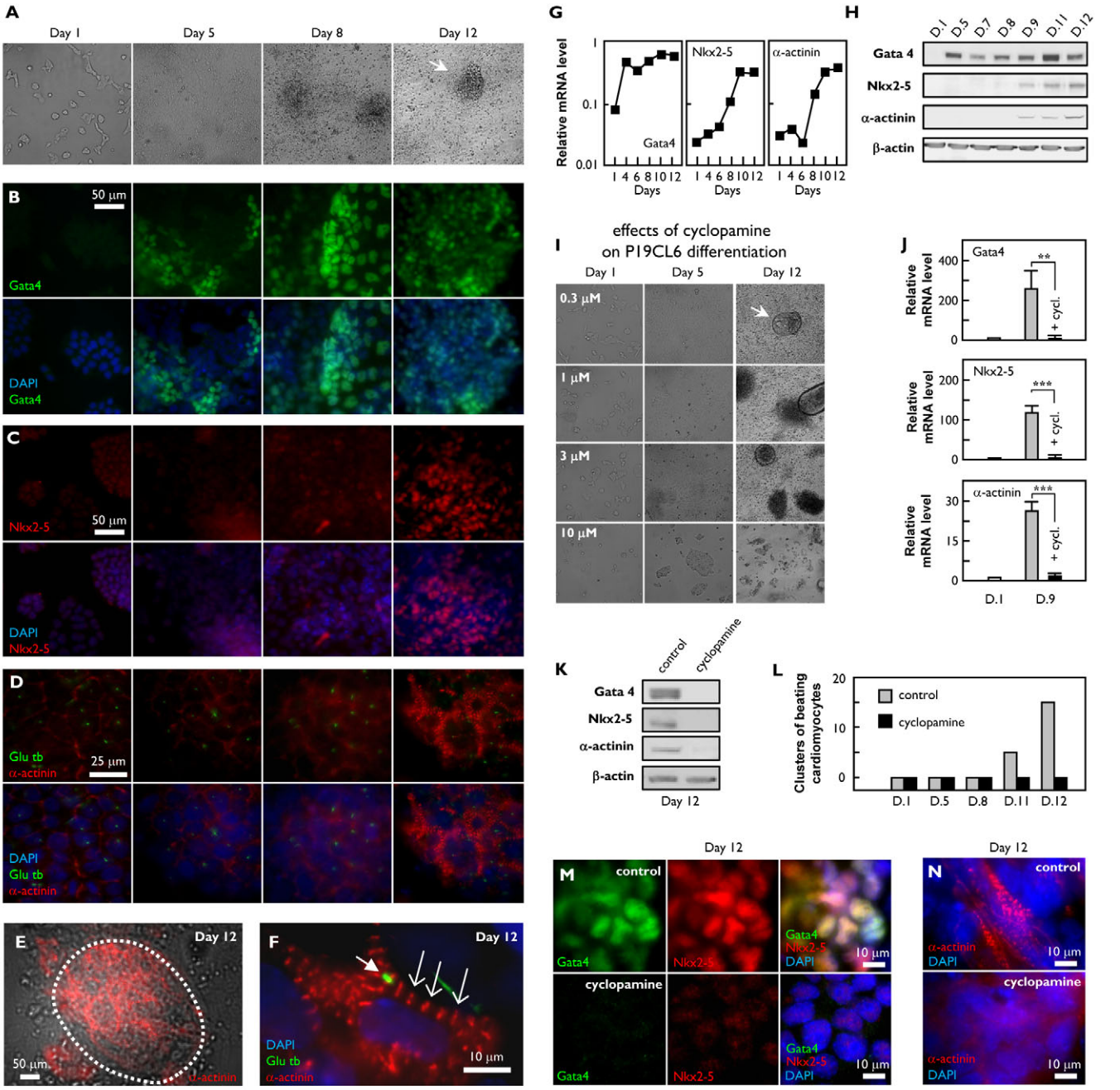

Fig. 1. Morphology of P19.CL6 cells during cardiomyocyte differentiation and the effect of cyclopamine on heart transcription factors. (A) Light microscope images of P19.CL6 cell morphology during differentiation at day 1, 5, 8 and 12. Arrow indicates a cluster of beating cardiomyocytes. (B) Immunofluorescence microscopy (IF) analysis of Gata4 localization at day 1, 5, 8, 12 (Gata4, green; DAPI, blue). (C) IF analysis of Nkx2-5 localization at day 1, 5, 8 and 12 (Nkx2-5, red) DF. (D) IF analysis of α-actinin and glutaminated tubulin at day 1, 5, 8, and 12 (α-actinin, red; Glu tb, green). (E) IF analysis of α-actinin localization merged with light microscope image of beating cardiomyocyte cluster at day 12 (α-actinin, red; dotted line marks edge of cluster). (F) High magnification of cardiomyocyte cell at day 12 (arrow indicates primary cilium; open arrow, Z-line in α-cardiac muscle stress fibers). (G) Quantitative RT-PCR analysis of Gata4, Nkx2-5 and α-actinin relative mRNA levels (data from one representative experiment of $n>3$). (H) Western blot analysis (WB) of anti-Gata4 (~53 kDa), Nkx2-5 (~40 kDa), α-actinin (~100 kDa) and β-actin (~43 kDa) reactivity on P19.CL6 cells at day (D) indicated. (I) Light microscope images of P19.CL6 cell morphology during differentiation at day 1, 5, and 12 with added 0.3, 1, 3 or 10 μM cyclopamine. Arrow indicates beating cluster of cardiomyocytes. (J) Quantitative RT-PCR analysis on Gata4, Nkx2-5 and α-actinin relative mRNA levels at day 1 and 9 in control and 3 μM cyclopamine-treated P19.CL6 cells. $^{**}P<0.01$; $^{***}P<0.001$. (K) WB analysis using anti-Gata4 (~53 kDa), Nkx2-5 (~40 kDa), α-actinin (~100 kDa) and β-actin (~43 kDa) on P19.CL6 cells at day 12 in control and 3 μM cyclopamine treated P19.CL6 cells. (L) Bar graph showing number of beating cardiomyocyte clusters at day 1, 5, 8, 11 and 12. Data from one representative experiment are shown. (M,N) IF analysis of Gata4 and Nkx2-5 localization (M) at day 12 in control and 3 μM cyclopamine-treated P19.CL6 cells (Gata4, green; Nkx2-5, red; DAPI, blue). (N) α-actinin localization at day 12 in control and 5 μM cyclopamine-treated P19.CL6 cells (α-actinin, red; DAPI, blue).

clusters of cardiomyocytes at day 12 on average in a 9.6 cm^2 culture dish (Fig. 1A,L). At this time point, the individual clusters had a diameter of 0.2-0.6 mm and the clusters could be observed in small networks beating synchronously at a frequency of about 60 rhythmic contractions per minute. Comparable structures of cardiogenic cell clusters were observed in differentiating P19.SI cells, another

subclone of P19 cells, which contracted synchronically by about 2 weeks (Angello et al., 2007). The network between clusters in differentiated P19.CL6 cells later develop into a thick unified layer of cardiac muscle epithelium (data not shown). Analysis of Gata4 and Nkx2-5 by immunofluorescence microscopy (Fig. 1B-C), showed that Gata4-positive cells were present from day 2 onwards during cardiomyocyte differentiation. Nkx2-5-positive cells appeared at a later stage (~day 9) during cardiomyogenesis. To verify that the P19.CL6 cells form cardiomyocytes, we stained with an antibody against the cardiomyocyte marker α-actinin, which localizes in the Z-line on α-cardiac muscle stress fibers (Fig. 1D-F). The structural organization of P19.CL6 cardiomyocyte muscle fibers takes place at approximately day 12. Primary cilia, localized with anti-detyrosinated tubulin (Glu-tub), label cells that have entered growth arrest (Satir and Christensen, 2007) and were present at all stages of heart development (Fig. 1D-F). This was particularly prominent in cells that had formed contact with other cells, either as confluent monolayers before the beginning of differentiation or as multilayered cell clusters during the subsequent phases of differentiation and formation of the beating cardiomyocyte. mRNA levels of Gata4, Nkx2-5 and α-actinin were analyzed by quantitative RT-PCR (Q-PCR) (Fig. 1G) and showed an increase over the 2 week growth period that matched the appearance of positive cells observed by immunofluorescence microscopy. As a control, the protein levels of Gata4, Nkx2-5 and α-actinin in western blot (WB) analysis (Fig. 1H), followed the increase in mRNA levels and localization intensities of the proteins upon immunofluorescence analysis; Gata4 expression was upregulated after day 2 and Nkx2-5 and α-actinin at around day 9. The effect of cyclopamine on P19.CL6 morphology indicated that a concentration of 0.3 μM of this Smo inhibitor was too low to suppress cardiomyocyte development (Fig. 1I). However, at cyclopamine concentrations above 1 μM, there were no beating clusters of cardiomyocytes, and at 10 μM or more, the cyclopamine became toxic and affected cell viability. Furthermore, cyclopamine concentrations equal to or greater than 1 μM altered the cell morphology in the culture and the cells aggregated in disorganized clusters that adhered poorly to the culture dish. The addition of 3 μM cyclopamine to the culture medium had a significant negative effect on the mRNA levels of Gata4, Nkx2-5 and α-actinin at day 9, compared with levels in control cells (Fig. 1J). A similar reduction in mRNA expression of the cardiomyocyte markers was observed at day 12 (data not shown). Furthermore, cyclopamine significantly reduced the protein levels of Gata4, Nkx2-5 and α-actinin in cells analyzed at day 12 (Fig. 1K), indicating an inhibition of cardiomyogenesis. Normal cardiomyocyte formation took place on average at day 12, whereas upon addition of 3 μM cyclopamine, we never observed any beating clusters of cardiomyocytes (Fig. 1L). There were no Gata4- and Nkx2-5 positive cells when cells were treated with 3 μM cyclopamine (Fig. 1M). Furthermore, a diffuse α-actinin staining pattern was observed (Fig. 1N), with no α-cardiac muscle stress fibers, suggesting that the cardiomyocyte sarcomeres failed to develop in the presence of cyclopamine by inhibition of the Hh pathway.

Stem cell markers during P19.CL6 differentiation

To verify that DMSO promotes the differentiation of P19.CL6 cells into cardiomyocytes and not other cell lineages, we followed the shift in cellular expression of stem cell markers into Gata4-positive cells. Confirmation that all P19.CL6 cells remained undifferentiated at day 1 was made by immunofluorescence analysis using the transcription factors Sox2 and Oct4, both markers for undifferentiated cells (Pesce and Scholer, 2001; Masui et al., 2007). Both markers colocalized to the nuclei of all cells at day 1 (Fig. 2A), at which time no cells were positive for Gata4 (Fig. 1B; Fig. 2B, left panels). During differentiation at day 5 after DMSO

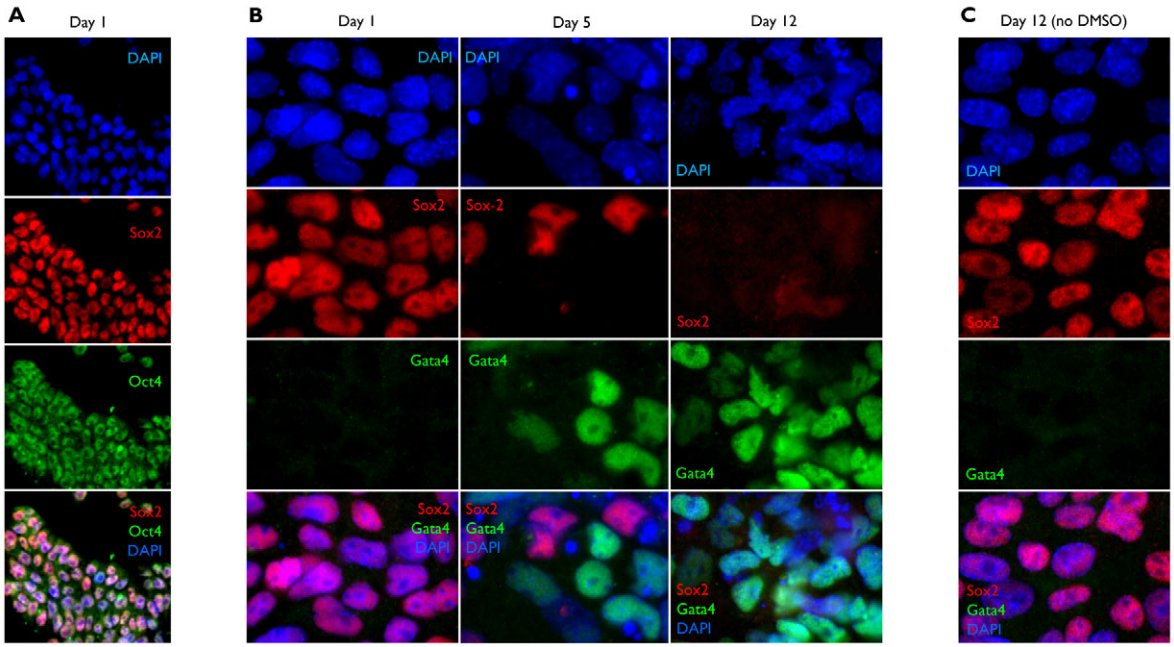

Fig. 2. Characterization of P19.CL6 stem cell lineage during cardiogenesis. (A) Immunofluorescence microscopy (IF) analysis of Sox2 and Oct4 localization at day 1 (Oct4, green; Sox2, red; DAPI, blue). (B) IF analysis of Sox2 and Gata4 localization at day 1, 5, 12 during differentiation in the presence of 1% DMSO (Gata4, green; Sox2, red; DAPI, blue). (C) IF analysis of Sox2 and Gata4 localization at day 12 in growth medium without 1% DMSO (Gata4, green; Sox2, red; DAPI, blue).

treatment, we observed a shift in the cellular expression of Sox2 to Gata4 such that cells were either Sox2 or Gata4 positive (Fig. 2B, middle panels). About 40% of the cells were Gata4 positive at this time point of differentiation. At day 12, the number of Gata4-positive cells increased to about 80%, whereas the remaining cells expressed Sox2 (Fig. 2B, right panels). As a control, all cells left in growth medium without DMSO for 12 days remained undifferentiated (Fig. 2C). These results show that DMSO primarily promotes the differentiation of P19.CL6 cells into cardiomyocytes and not other cell lineages.

Cyclopamine inhibits the Hedgehog signaling pathway and heart development in P19.CL6 cells

The results of cyclopamine treatment in P19.CL6 cells presented in Fig. 1 indicate that the Hh signaling pathway is turned off (Fig. 3) and that normal cardiogenesis requires the Hh signaling pathway to become activated, as previously suggested for P19 EC cells (Gianakopoulos and Skerjanc, 2005). Elevated mRNA levels of Gli1 and Ptc1 during P19.CL6 differentiation at day 9 were no longer apparent upon 3 μM cyclopamine treatment (Fig. 3A). The Hh transcription factor Gli2 exists in a full-length activator form (Gli2-A) and in repressor forms (Gli2-R), which are formed after C-terminal degradation of the protein (Pan et al., 2006). We here show that 3 μM cyclopamine at day 5 reduces the level of the full-length form of Gli2 (~160 kDa), as judged by WB analysis with an antibody directed against the internal region of Gli2 (Gli2-G20) that recognizes only the full-length form of Gli2 (Nielsen et al., 2008) (Fig. 3B). WB analysis was also performed at day 9 using an antibody directed against the N-terminal region of Gli2 (Gli2-N20), which recognizes processed forms of Gli2 (Nielsen et al., 2008). In this analysis Gli2-N20 detected a protein band at ~60 kDa, which increased in intensity in the presence of cyclopamine (Fig. 3C). Both protein bands were eliminated by addition of blocking peptide to the antibodies. These results might indicate that inhibition of Hh signaling by cyclopamine treatment is associated with processing of Gli2 into repressor forms, although further analysis will be required to identify their function in Hh signaling.

The effect of cyclopamine on Gli1 expression was also investigated by immunofluorescence analysis at day 2, 5 and 9 of differentiation. The level of Gli1 expression greatly increased in the nucleus at day 5 and 9 (Fig. 3D-F), and this increase was largely abolished in the presence of 3 μM cyclopamine. Confirmation that Gli1 increased in cells that differentiate into cardiomyocytes was made by immunofluorescence analysis, which showed colocalization of Gli1 and Nkx2-5 in cells at day 9 (Fig. 3G). Similarly, Gli2 and Gli3 expression levels at day 5 in the absence and in the presence of 3 μM cyclopamine was observed (Fig. 3H-I). We used Gli2 (G-20) and Gli3 (C-20) antibodies, which recognize the full-length forms of each transcription factor. In both cases, cyclopamine strongly reduced the nuclear localization of Gli2 and Gli3. These results support the conclusion that cyclopamine prevents P19.CL6 cells from differentiating into cardiomyocytes by shutting down Hh signaling in the early phases of differentiation.

Hedgehog signaling components localize to primary cilia in P19.CL6 cells

Hh signaling was previously suggested to be coordinated by primary cilia (Liu et al., 2005). To confirm formation of primary cilia in cultures of P19.CL6 cells, we initially performed immunofluorescence analysis using anti-pericentrin (Pctn), which

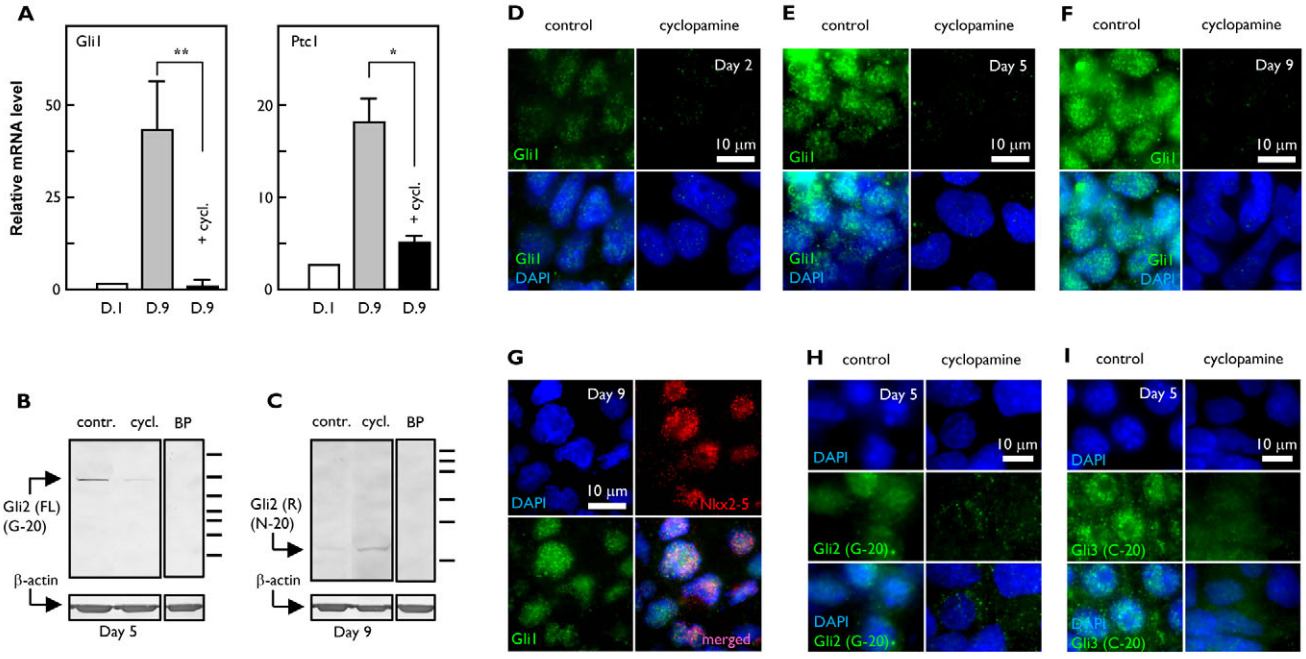

Fig. 3. Effect of cyclopamine on the Hh-signaling pathway in P19.CL6 cells. (A) Quantitative RT-PCR analysis of Ptc1 and Gli1. Relative mRNA levels on day 1 and 9 in control and 3 μM cyclopamine-treated P19.CL6 cells. *P<0.05; **P<0.01. (B,C) Western blot analysis using (B) anti-Gli2 (G-20 ~160 kDa) full-length and β-actin (~43 kDa) reactivity on P19.CL6 cells on day 5 (markers: 70, 80, 90, 100, 120, 160, 220 kDa), with a blocking peptide control (BP, 60× Ab concentration) and (C) anti-Gli2 (N-20 ~55 kDa) repressor and β-actin (~43 kDa) on day 9 (markers: 50, 60, 70, 80, 90, 100 kDa) with BP control. (D-F) Immunofluorescence microscopy (IF) analysis of Gli1 localization in control and 3 μM cyclopamine-treated P19.CL6 cells on day 2 (D), day 5 (E) and day 12 (F). Gli1, green; DAPI, blue. (G) IF analysis of Gli1 and Nkx2-5 localization on day 9. Gli1, green; Nkx2-5, red. (H,I) IF analysis of Gli2(G-20) (H) and Gli3(C-20) (I) localization on day 5 in control and 3 μM cyclopamine-treated P19.CL6 cells.

labels the centrosome, and anti-acetylated α-tubulin, which labels primary cilia in growth-arrested cells (Schneider et al., 2005). As shown in Fig. 4A, primary cilia were clearly observed in cells either in confluent monolayers or in multilayered cell clusters, as also indicated with Glu-tub in Fig. 1D-F. Co-localization studies with α-tubulin and antibodies directed against Ptc1, Smo and Gli2 showed that all three Hh components localize to the primary cilium as indicated in Fig. 4B-D. Immunofluorescence analysis showed the ciliary localization of Ptc-1 and Gli2 in cells expressing Gata4 and Nkx2-5, respectively (Fig. 4E-F), which confirms that Hh components localize to cilia in cells differentiating into cardiomyocytes. We also observed that the intensity of ciliary Ptc1 and Smo fluctuated in the cell cultures during cardiogenesis. This was particularly evident around the forming cell clusters, which tended to have more Smo and less Ptc1 in the cilium (data not shown). At the end stage of differentiation, however, we also observed that ciliary Ptc1 often increased in intensity in the cilium. These observations could indicate that the primary cilium in P19.CL6 cells is part of the signaling machinery that coordinates activation of the Hh pathway during differentiation, and that Ptc1 participates in a negative regulatory feedback inhibition in the developed cardiomyocytes. In this scenario, either newly expressed and/or pre-existing Ptc-1 might translocate to the primary cilium at the end stage of differentiation, although further analysis is required to examine the importance of changes in ciliary localizations of Hh components during differentiation of P19.CL6 cells into beating cardiomyocytes.

Knocking down the primary cilium with Ift88 and Ift20 siRNA prevents cardiogenesis

To investigate more directly the importance of primary cilia in early cardiogenesis, we investigated the effects of knockdown of Ift88/Polaris and Ift20 on differentiation of P19.CL6 cells into cardiomyocytes. Using antibodies against Ift88 and Ift20 (Fig. 5A) we initially observed that Ift88 predominantly localizes to the ciliary base and tip, whereas Ift20 had a centrosome and Golgi localization at the primary cilium in P19.CL6 cells. This localization is identical to that observed in other cell types (Pazour et al., 2000; Taulman et al., 2001; Follit et al., 2006; Haycraft et al., 2005). Confirmation that Ift88 and Ift20 localized to the cilia, centrosome and Golgi in cells that differentiate into cardiomyocytes was made by immunofluorescence analysis, which showed localization of both IFT proteins in cells that express Nkx2-5 at day 9 (Fig. 5B).

For knockdown studies, we nucleofected cells either with a siRNA construct targeting Ift88 alone or in combination with a siRNA construct targeting Ift20 (Ift88+Ift20); the Ift88 construct expresses GFP. Then, we followed the effect of the knockdown constructs on expression rates of Ift88 and Ift20, assembly rates of primary cilia, expression rates of Gata4, Nkx2-5 and α-actinin, and rates of beating cardiomyocytes. Using Q-PCR analysis, we found that Ift88 and Ift88+Ift20 knockdown reduced the level of Ift88 mRNA to about 50% compared with mock-transfected cells under both conditions 3 days after nucleofection (Fig. 5C). Ift20 mRNA was reduced to about 25% when transfected with Ift88+Ift20 siRNA but it was not affected by Ift88 nucleofection alone. These results indicate that Ift88 siRNA does not affect the expression of Ift20 and vice versa. Furthermore, western blot analysis showed that the protein levels of Ift88 (~95 kDa) and Ift20 (~16 kDa) are significantly reduced by siRNA nucleofection (Fig. 5D). As a control for the Ift88 antibody, we performed western blot analysis on NIH3T3 cells, wt MEFs and *Ift88*^{Tg737NRpw} MEFs (*Tg737*^{orpk} MEF) showing that the Ift88 protein band at 95 kDa is absent in mutant fibroblasts (Fig. 5E). This has also been reported in *prx1cre;Ift88*$^{fl/n}$ conditional mutants (Haycraft et al., 2007). Immunofluorescence analysis was performed to show that cells nucleofected with the Ift88 siRNA construct expressing GFP grew no or very short cilia (<1 μm) compared with mock-transfected cells, which formed cilia of ~4 μm in length (Fig. 5F). Furthermore, in mock-transfected cultures, about 70% of the cells formed primary cilia, which was reduced to about 30% in Ift88-transfected cells (Fig. 5G). A combination of both Ift88 and Ift20 siRNA reduced the frequency of ciliated cells further to about 20%.

Q-PCR analysis demonstrated that knockdown of the primary cilium was associated with a reduction of mRNA expression rate of Gata4 to about 40% and 25% relative to mock-transfected cells with Ift88 and Ift88+Ift20 siRNA, respectively (Fig. 6A). Immunofluorescence analysis confirmed that cells nucleofected with the Ift88 siRNA construct expressing GFP were Gata4 negative (Fig. 6B) and Sox2 positive (Fig. 6C), indicating that knockdown of the primary cilium maintains cells in their undifferentiated state. In

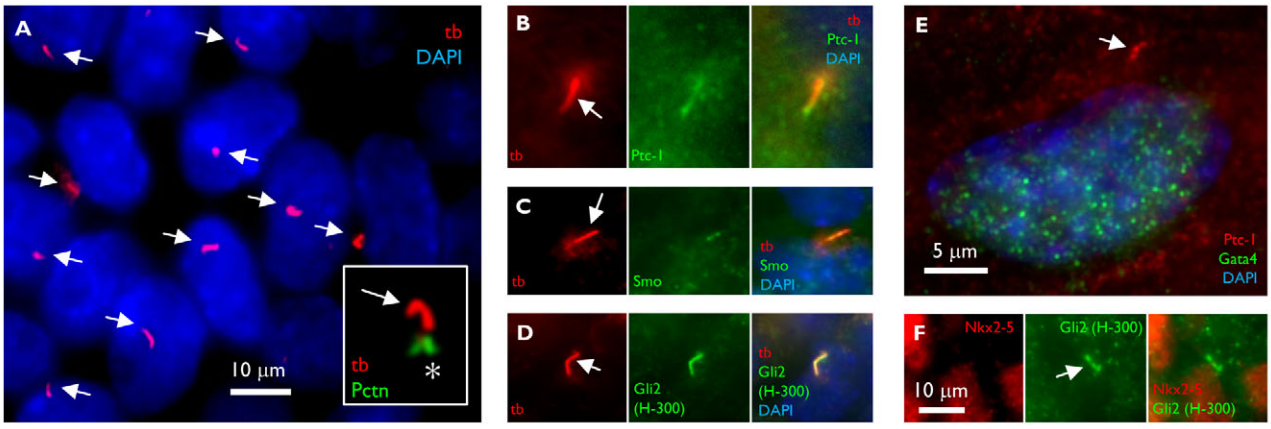

Fig. 4. Ciliary localization of Hh-signaling components in P19.CL6 cells. (A) Immunofluorescence microscopy (IF) analysis of acetylated tubulin (tb) on primary cilia after 24 hours (tb, red; pericentrin, green; DAPI, blue). Asterisk indicates centrosome region and arrows show primary cilium. (B) IF analysis of Ptc1 localization to the primary cilium. (C) IF analysis of Smo localization to the primary cilium. (D) IF analysis of Gli2 localization to the primary cilium. (E) IF analysis of Ptc-1 and Gata4 localization at day 12. (F) IF analysis of Gli2(H-300) and Nkx2-5 localization at day 12. Arrows in B-F indicate the primary cilium.

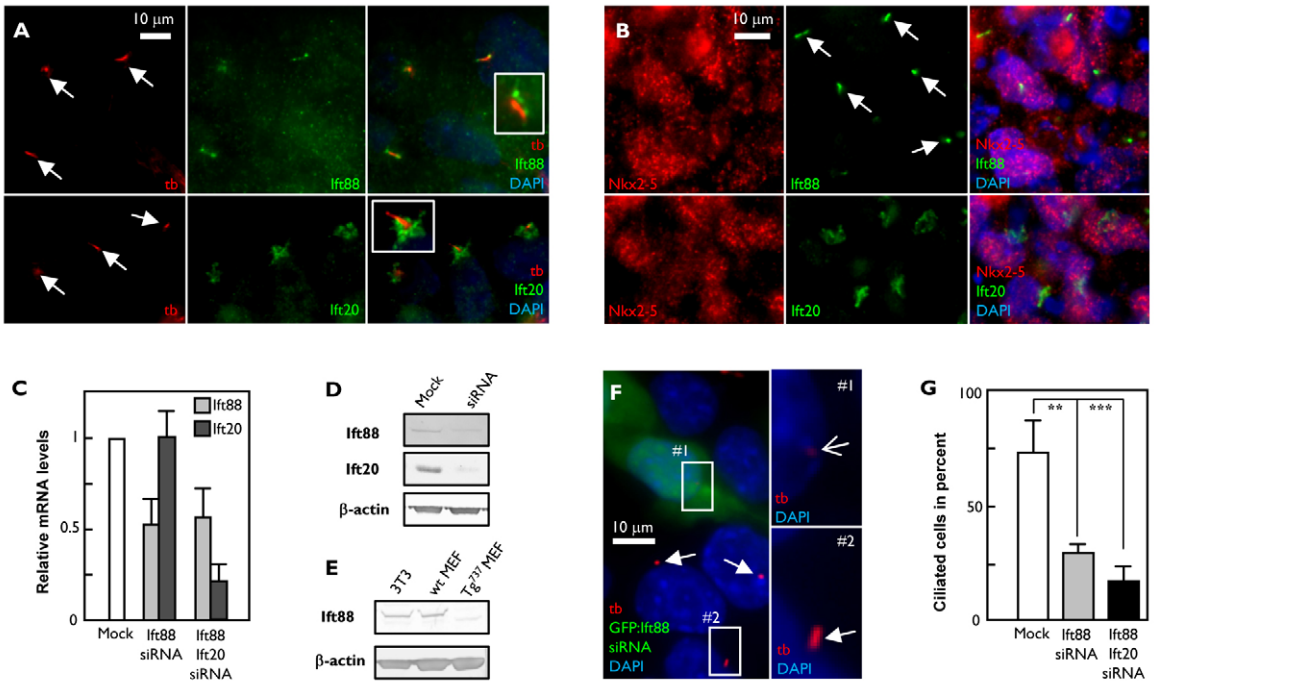

Fig. 5. Ift88 and Ift20 knockdown by siRNA nucleofection in P19.CL6 cells. (A) Immunofluorescence microscopy (IF) analysis of Ift88 (top panel) and Ift20 protein (bottom panel) localization in P19.CL6 cells [Ift88+Ift20, green; acetylated tubulin (tb), red; DAPI, blue]. (B) Localization of Ift88 and Nkx2-5 (top panel) and Ift20 and Nkx2-5 (bottom panel) in P19.CL6 cells (Ift88 and Ift20, green; Nkx2-5, red; DAPI, blue). Arrows in A,B indicate primary cilium. (C) Quantitative RT-PCR analysis on Ift88 and Ift20 relative mRNA levels after Ift88 and Ift88+Ift20 siRNA nucleofection vs mock treatment after 72 hours. (D) Western Blot (WB) analysis on day 5 of Ift88 (~95 kDa), Ift20 (~16 kDa) and β-actin (~43 kDa) reactivity on P19.CL6 cells after Ift88+Ift20 siRNA nucleofection vs mock treatment. (E) WB analysis of Ift88 (~95 kDa) and β-actin (~43 kDa) reactivity on NIH3T3, wt and ORPK (*Tg737*^{orpk}, *Ift88*^{Tg737Rpw}) MEF cells after 24 hours of serum starvation. (F) IF analysis of acetylated tubulin localization combined with GFP-Ift88-siRNA nucleofection (GFP-Ift88 siRNA, green; tb, red; DAPI, blue). Arrows indicate primary cilium; open arrow indicates missing primary cilium. (G) Bar graph showing the percentage of ciliated cells in mock, Ift88 and Ift88/Ift20 siRNA nucleofected cells after 24 hours. $^{**}P<0.01$; $^{***}P<0.001$.

addition, Ift88+Ift20 siRNA effectively blocked expression and nuclear localization of Gata4 (Fig. 6D). Similarly, Q-PCR and western blot analysis showed that Ift88+Ift20 siRNA reduced the mRNA and/or protein levels of Nkx2-5 and α-actinin at day 9 (Fig. 6E,F). Finally, we analyzed the number of clusters of beating cardiomyocytes after addition of siRNA (Fig. 6G). The cultures were scanned daily for beating clusters; day [X] marking the day of the first observed beating cluster in a 9.6 cm^2 culture dish. The cells were then recounted for beating clusters the day after [X+1]. The time point for formation of beating clusters could vary a few days from one experiment to another, although all experiments showed beating clusters, on average, at day 12. In a screen of more than eight independent experiments, we observed no major differences in the time point for appearance of beating clusters in mock-treated versus non-treated cells. As shown in Fig. 6G, both Ift88 and Ift88+Ift20 siRNA reduced the number of beating cardiomyocytes from about 12 beating clusters in mock-transfected cells to about 3 and 1.5 beating clusters on average in Ift88 and Ift88+Ift20 siRNA nucleofected cells, respectively, at day X+1. The size of the beating clusters in siRNA nucleofected cells was reduced to about 20% of the size of clusters in mock-transfected cells, and no networks were observed between individual clusters. These results support the conclusion that primary cilia are crucial regulators of P19.CL6 cardiogenesis.

Knockdown of Ift88 and Ift20 blocks Hedgehog signaling

To further investigate the significance of primary cilia in coordination of Hh signaling in P19.CL6 cardiogenesis, we initially analyzed the effect of Ift88+Ift20 siRNA on the expression levels of Ptc1 mRNA (Fig. 7A) and Gli1 mRNA (Fig. 7B) at day 5 of differentiation by Q-PCR analysis. In both cases, knockdown of the cilium largely reduced the expression levels of both Hh signaling markers to about 12% and 4%, respectively, relative to mock-transfected cells. Immunofluorescence analysis demonstrated that Ift88+Ift20 siRNA blocked the expression and nuclear localization of Gli1 at day 5 (Fig. 7C), which was comparable with that observed in the presence of cyclopamine (Fig. 3E). Therefore, the primary cilium might control P19.CL6 cardiogenesis partly by coordinating the Hh signaling machinery.

Heart defects in E11.5 Ift88-null mice

The Ift88-null (*Ift88*^{tm1Rpw}, *Ift88*$^{-/-}$) mouse has multiple developmental phenotypes including random left-right axis specification, neural tube closure and patterning abnormalities, hepatic and pancreatic ductal defects, polydactyly, cerebellar hypoplasia and retinal degeneration because of malfunctioning or loss of primary cilia (Lehman et al., 2008). Since knockdown of Ift88 severely inhibits cardiomyogenesis in P19.CL6 cells (Fig. 6), we hypothesized that the loss of Ift88 in *Ift88*^{tm1Rpw} (*Ift88*$^{-/-}$) mice would cause heart defects. This hypothesis was tested by investigating cardiac tissue sections from WT and *Ift88*$^{-/-}$ embryos at day E11.5 (Fig. 8). In the embryonic hearts of homozygous *Ift88*$^{-/-}$ mice (Fig. 8A,B), we observed malformations of the cardiac outflow tract (OFT) and the ventricles. The length of the distal truncus in *Ift88*$^{-/-}$ mice was significantly shorter compared with

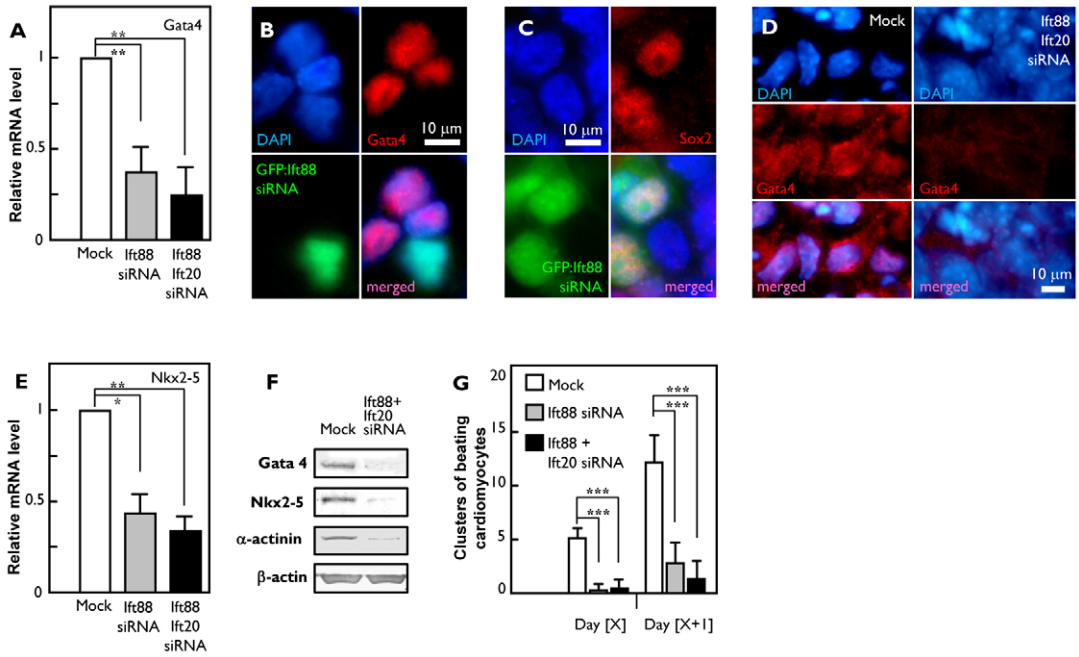

Fig. 6. Effect of Ift88 and Ift20 knockdown by siRNA nucleofection on cardiomyocyte formation in P19.CL6 cells. (A) Quantitative RT-PCR analysis on Gata4 relative mRNA levels after nucleofection with Ift88 siRNA alone or with Ift88+Ift20 siRNA vs mock control on day 5. (B) IF analysis of Gata4 expression in Ift88 nucleofected P19.CL6 cells, 72 hours after nucleofection (GFP-Ift88 siRNA, green; Gata4, red; DAPI, blue). (C) IF analysis of Sox2 expression in Ift88 nucleofected P19.CL6 cells 72 hours after nucleofection (GFP-Ift88 siRNA, green; Sox2, red; DAPI, blue). (D) IF analysis of Gata4 expression in Ift88+Ift20 nucleofected cells vs mock control at day 5 (Gata4, red; DAPI, blue). (E) Quantitative RT-PCR analysis on Nkx2-5 relative mRNA levels after Ift88 and Ift88+Ift20 siRNA nucleofection vs mock control at day 5. (F) WB analysis of Gata4 (~53 kDa, day5), Nkx2-5 (~40 kDa, day 12), α-actinin (~100 kDa, day 12) and β-actin (~43 kDa) reactivity on P19.CL6 cells after Ift88+Ift20 siRNA nucleofection vs mock control. (G) Number of beating cardiomyocyte clusters in mock, Ift88 and Ift88+Ift20 nucleofected P19.CL6 cells. Day [X] symbolizes the first day where beating clusters were observed in a culture, the cultures were recounted on the following day (Day [X+1]). *P<0.05; **P<0.01; ***P<0.001.

that of WT mice, and the OFT cushions seemed to be malformed, with a thinner appearance (Fig. 8A). The WT mice had expanded cardiac cushion tissue and a distinct transformation of endocardial cells into mesenchyme, whereas the epithelial-mesenchymal transformation (EMT) was virtually absent in the *Ift88*$^{-/-}$ mice. The ventricles of *Ift88*$^{-/-}$ mice appeared dilated and empty because of greatly reduced ventricular trabeculation compared with that in WT mice (Fig. 8B). Furthermore, there was an increased volume of the pericardial space in the *Ift88*$^{-/-}$ embryo compared with that of the WT embryo (arrowheads in Fig. 7B). We verified that the mouse embryos were of the correct genotype (Fig. 8C) and immunohistochemical analysis showed that the Ift88-null mice had no or very short primary cilia, as expected (Fig. 8D). Immunohistochemical analysis also showed that Gli2 localizes to primary cilia in the developing heart of WT embryos, such as in the ventricular body wall (Fig. 8E, top panel). This localization is absent in *Ift88*$^{-/-}$ embryos (Fig. 8E, bottom panel). These in vivo findings support the conclusion that primary cilia have an important role in cardiogenesis by coordinating Hh signaling.

Discussion

Primary cilia have a critical role in the coordination of a number of developmental processes in mammals, such as embryonic left/right determination, skeletal patterning, limb formation and neurogenesis (Nonaka et al., 1998; Gouttenoire et al., 2007; Haycraft et al., 2007; Breunig et al., 2008). Brueckner and co-workers (Slough et al., 2008) demonstrated that E9.5 *Kif3a*$^{-/-}$ mouse embryos have abnormal development of ECCs and reduced trabeculation, indicating that primary cilia in the heart could regulate processes in cardiac morphogenesis, because Kif3a is required for ciliary assembly amongst other cellular functions (Slough et al., 2008). Here, we studied the function of the primary cilium in early cardiogenesis by examining differentiated clusters of cardiomyocytes, and by analysis of defects in heart development in Ift88-null E11.5 mouse embryos, which form no or very short primary cilia.

Primary cilia in P19.CL6 stem cell differentiation

P19.CL6 stem cells spontaneously differentiate into clusters of beating cardiomyocytes in the presence of DMSO (Habara-Ohkubo, 1996). We show that P19.CL6 stem cell form primary cilia and that essential components of the Hh pathway, Ptc1, Smo and Gli2, localize to P19.CL6 cilia. This is the first discovery of primary cilia in this cell line. Before cardiomyocyte differentiation, the cells are kept in their pluripotent state, as evidenced by expression of the stem cell markers Sox2 and Oct4. Inhibition of the Hh pathway by cyclopamine blocks DMSO-induced differentiation of P19.CL6 cells into clusters of beating cardiomyocytes by obstructing the expression and nuclear localization of the heart transcription factors Gata4 and Nkx2-5, which mark early cardiomyocyte differentiation (Grepin et al., 1997; Lints et al., 1993). Further, cyclopamine altered the cell morphology; cells aggregated in disorganized clusters associated with a decreased expression of α-actinin and a lack of α-actinin organized into the Z-line on α-cardiac muscle stress fibers, which indicate fully differentiated cardiomyocytes. The inhibitory effect of cyclopamine on Hh signaling in P19.CL6 cells was

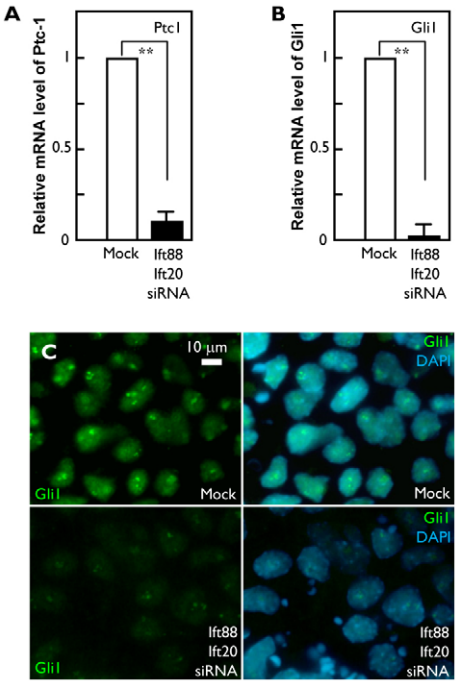

Fig. 7. Effect of knockdown of Ift88 and Ift20 on Hh signaling in P19.CL6 cells. (A,B) Quantitative RT-PCR analysis of Ptc1 (A) and Gli1 (B) relative mRNA levels after Ift88+Ift20 siRNA nucleofection vs mock control on day 5. (C) Immunofluorescence microscopy analysis of Gli1 expression in Ift88-Ift20 nucleofected P19.CL6 cells compared with mock control on day 5 (Gata4, green; DAPI, blue). $^{**}P<0.01$.

confirmed by inhibition of DMSO-induced upregulation of Gli1 and Ptc1 mRNA expression and nuclear localization of Gli1, Gli2 and Gli3. In support of the conclusion that cyclopamine inhibits Hh signaling by processing of Gli2, we used western blot analysis to show that the level of the full-length form of Gli2, which might function as an activator form of Gli2, is reduced in cyclopamine-treated cells. Concomitantly, in the presence of cyclopamine, we observed an increase in a processed form of Gli2, which might represent an inhibitory form of Gli2 (Pan et al., 2006). These results confirm that Hh signaling is required for differentiation of P19.CL6 cells into cardiomyocytes, and that Hh signaling may be associated with primary cilia in P19.CL6 cells.

To determine the function of the primary cilium in regulation of Hh signaling and in cardiomyogenesis, we carried out experiments in which the primary cilium was knocked down by Ift88 and Ift20 siRNA. Initially, we showed that Ift88 uniquely localizes to primary cilia and that Ift20 localizes to the centrosome and Golgi region in P19.CL6 cells, as previously shown in differentiated cells (Pazour et al., 2000; Follit et al., 2006; Haycraft et al., 2005). Ift88 is a subunit of the IFT particle complex B and is required for functional IFT and ciliary assembly (Pazour et al., 2000; Lucker et al., 2005). Ift20 functions in the delivery of ciliary membrane proteins from the Golgi complex to the cilium and strong knockdown of this IFT particle blocks ciliary assembly without affecting Golgi structure (Follit et al., 2006). Ift20 is anchored to the Golgi complex by the golgin protein GMAP210, and mice lacking GMAP210 die at birth with a pleiotropic phenotype that includes ventricular septal defects of the heart, although cells have normal Golgi structure (Follit et al., 2008). Knockdown of Ift88 in P19.CL6 cells reduced the frequency of ciliated cells by more than 50% and inhibited the expression levels of both Gata4 and Nkx2-5 to about 40% at day 5 of transfection, and this was associated with a decrease in nuclear localization of Gata4 followed by a reduced number of beating cardiomyocytes at around day 12. We also observed that cells transfected with Ift88 siRNA were Sox2 positive, indicating that knockdown of the cilium maintains cells in their undifferentiated state and the cells then do not undergo apoptosis or differentiate into other cell lineages. We next performed double knockout of Ift88 and Ift20 to show that an augmented reduction of primary cilia is associated with an additional decrease in mRNA expression levels of Gata4 and Nkx2-5 and numbers of clusters of beating cardiomyocytes in accordance with a strong reduction in protein levels of Gata4, Nkx2-5 and α-actinin. Since knockdown of Ift88 and Ift20 produces an inhibitory response on Hh signaling that is similar to that of cyclopamine in P19.CL6 cells at day 5 of differentiation (i.e. strongly reduces the expression levels of Ptc1 and Gli1 as well as the nuclear localization of Gli1), we conclude that differentiation of P19.CL6 cells into cardiomyocytes is governed by the primary cilium, partly by regulation of Hh signaling.

A number of observations have indicated a crucial function of primary cilia in differentiation processes in mammalian stem cells. Human embryonic stem cells (hESCs) possess primary cilia (Kiprilov et al., 2008) that contain a series of signal transduction components, including PDGFRα (Awan et al., 2009) and members of the Hh and Wnt signaling systems (Awan et al., 2009; Kiprilov et al., 2008), which are important in stem cell maintenance, differentiation and proliferation. It was further shown that primary cilia are crucial for the development of neural stem cells needed for proper development of the hippocampal region (Han et al., 2008) and in development of the neocortex and cerebellum (Spassky et al., 2008). These results imply that stem cell primary cilia per se might coordinate cellular processes in early development, including cardiogenesis. The mechanism by which Ptc1, Smo and Gli2 coordinate Hh signaling in the cilium of P19.CL6 is presently not understood. Our preliminary data suggest that Ptc1 and Smo become differentially localized to the cilium during the differentiation stages towards formation of beating cardiomyocytes, as previously described for cilia after stimulation of the Hh pathway in hESCs, fibroblasts, MDCK cells and epithelial cells from the exocrine ducts of the human pancreas (Haycraft et al., 2005; Huangfu and Anderson, 2005; Liu et al., 2005; May et al., 2005; Rohatgi et al., 2007; Nielsen et al., 2008). The regulated movement of Ptc1 out of the cilium and Smo into the cilium might create a switch by which cells can regulate Gli processing and turn Hh signaling on (reviewed by Christensen and Ott, 2007). Further experiments are required to investigate this in detail to understand how the primary cilium might function as a specialized organelle that integrates positive and negative inputs on Hh signaling in P19.CL6 cell differentiation.

Primary cilia are important for cardiogenesis in vivo

The cardiac phenotype of E11.5 *Ift88*$^{-/-}$ embryos, where ciliogenesis is inhibited, resembles in part, the cardiac phenotypes of *Pkd2*$^{-/-}$ and *Kif3a*$^{-/-}$ mice (Slough et al., 2008), which have malformed endocardial cushions, decreased trabeculation and increased pericardial space. Slough et al. (Slough et al., 2008) showed, by comparison to *lrd*$^{-/-}$ embryos, that decreased trabeculation and increased pericardial space are not related to abnormal development of the left-right asymmetry, which is initiated at the node of the

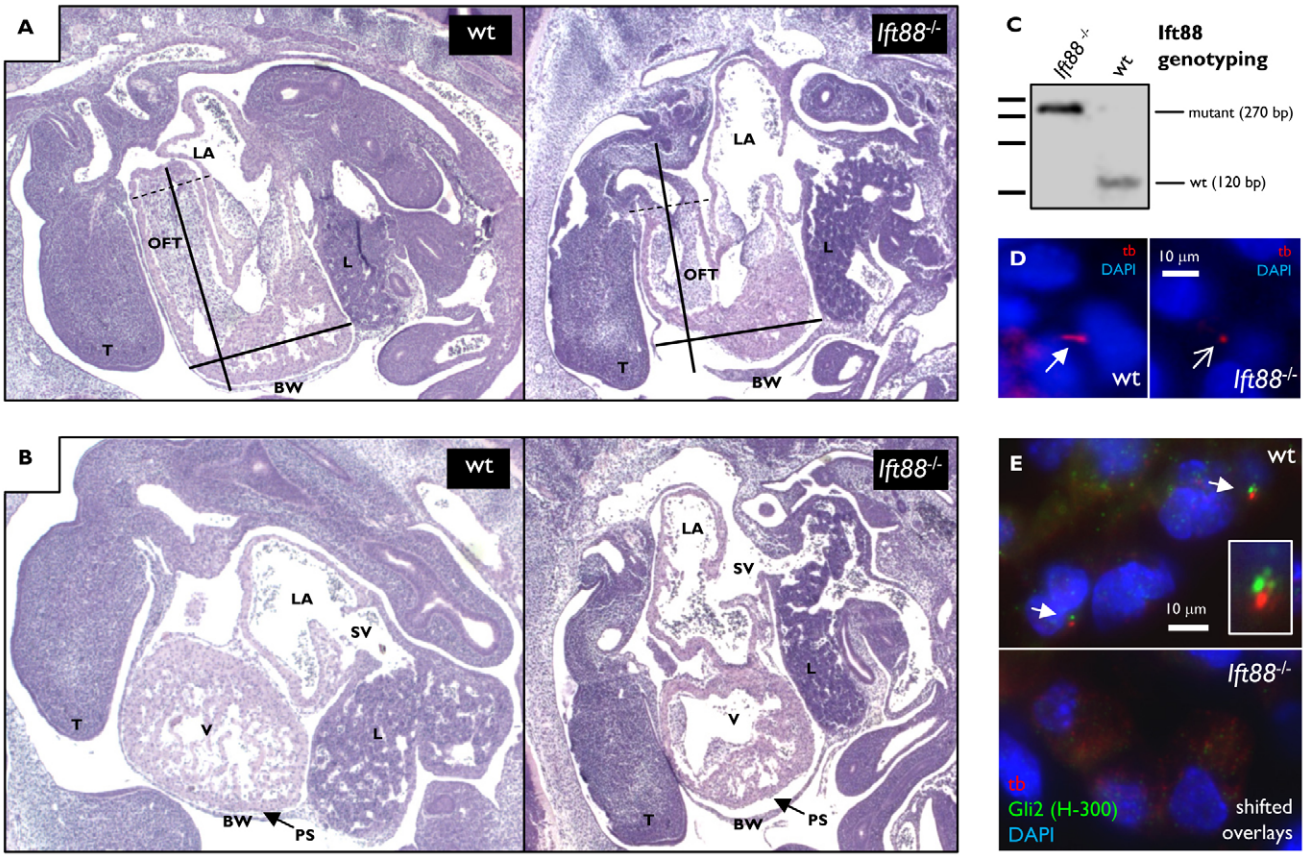

Fig. 8. Cardiac morphology of WT and *Ift88*^{tm1Rpw}-null embryos. (A) Comparable 3-μm-thick longitudinal mid-saggital sections of E11.5 WT and *Ift88*^{tm1Rpw} (*Ift88*$^{-/-}$) embryos. BW, body wall; L, liver; LA, left atrium; OFT, outflow tract; PS, pericardial space (arrowhead); SV, sinus venosus; T, tongue; V, ventricle. (B) Comparable 3-μm-thick longitudinal parasagittal sections of day E11.5 WT and Ift88-null mice. Arrowheads indicate the pericardial space (PS), which is extended in Ift88-null mouse. The black bars have identical dimensions in A and B. The distal end of the OFT are marked with a dotted line. (C) Genotyping of E11.5 WT and Ift88-null mice. Wild-type samples have a 120 bp band whereas Ift88-null has a 270 bp band. (D) Immunofluorescence microscopy analysis of acetylated tubulin (tb) on primary cilia in the heart of E11.5 WT and Ift88-null mice (tb, red; DAPI, blue). Arrow indicates primary cilium and open arrow shows missing primary cilium. (E) Immunofluorescence microscopy analysis of Gli2(H-300) and acetylated tubulin (tb) on primary cilia in the heart of WT and Ift88-null mice (tb, red; DAPI, blue). Arrow indicates primary cilium.

mouse at E7.75 and coordinated by nodal cilia. Therefore, our results on the *Ift88*$^{-/-}$ mouse support these findings (Slough et al., 2008) and suggest that these defects in cardiac morphogenesis are not caused by defects in nodal cilia, but in cardiac primary cilia in the developing heart. We also show that that *Ift88*$^{-/-}$ E11.5 embryos have malformations of the cardiac outflow tract (OFT), indicating that primary cilia also have an essential role in formation of the OFT. Brueckner and colleagues (Slough et al., 2008) did not investigate OFT malformations.

A series of signal transduction pathways have been implicated in the morphogenesis of the embryonic heart after establishment of the left-right asymmetry, some of which could be coordinated by the cardiac primary cilium. Our in vitro data on P19.CL6 cells show that Hh signaling is one of the ciliary pathways necessary for cardiomyocyte differentiation, and we surmise that ciliary Hh signaling in a similar manner coordinates in vivo morphogenesis of the heart. As an example, Gli2 localizes to primary cilia in both P19.CL6 cells and in the developing heart of WT embryos, and this localization is disrupted in *Ift88*$^{-/-}$ embryos. Interestingly, the OFT phenotype of *Ift88*$^{-/-}$ embryos resembles that of *Shh*$^{-/-}$ mice (Washington Smoak et al., 2005; Goddeeris et al., 2007), suggesting that aberrant Hh signaling due to defects in assembly of primary cilia is involved in shortening of the OFT and potentially in other cardiac structures in *Ift88*$^{-/-}$ embryos. Indeed, cardiac expression of *Nkx2-5* during heart development is blocked in the *Smo*$^{-/-}$ mouse embryo at the 2- to 3-somite stage (which corresponds to E9), suggesting that *Nkx2-5* is a specific cardiac target of Hh signaling and when blocked, underlies the defective heart morphogenesis observed in *Smo* mutants (Zhang et al., 2001). Similarly, our results show that knockdown of the primary cilium in P19.CL6 cells inhibits Hh signaling and blocks the expression of *Nkx2-5*, supporting the conclusion that primary cilia have an important role in heart development, in part by coordinating Hh signaling. Whether the primary cilium regulates cardiogenesis by coordinating other signaling pathways, such as Wnt, BMP and PDGF signaling, is presently unknown. Wnt and PDGF signaling are regulated by the cilium in a series of other cell types involved in growth control, migration and differentiation (reviewed by Christensen et al., 2008; Gerdes and Katsanis, 2008). BMP promotes the induction of cardiomyocytes from the mouse stem cell line P19.SI (Angello et al., 2007) and human embryonic stem cells (Takei et al., 2009). Based on their findings on *Pkd2*$^{-/-}$ mouse embryos, Slough and colleagues (Slough et al., 2008) also hypothesized that primary cilia in the heart and/or vasculature can function as mechanosensors to

detect blood flow essential for cardiac morphogenesis. In this regard, GMAP210 and Ift20 might function together at the Golgi in the sorting or transport of polycystin-2 to the ciliary membrane (Follit et al., 2008). Furthermore, primary cilia on endothelial cells (ECs) in blood vessels might function as laminar shear stress sensors to maintain heart homeostasis (Iomini et al., 2004). Cilia in cultures of embryonic ECs contain polycystin-1, which when subjected to shear stress, is cleaved, leading to changes in cellular signaling processes (Nauli et al., 2008). These results support the conclusion that primary cilia have a major role during development and in homeostasis of the heart.

We show here that primary cilia are crucial for coordination of early cardiogenesis. Knockdown of Ift88 and Ift20 blocks assembly of primary cilia and differentiation of P19.CL6 stem cells into clusters of beating cardiomoycytes. Knockout of Ift88 and defective assembly of primary cilia in the E11.5 *Ift88*$^{-/-}$ mouse lead to cardiac malformation, most probably as a consequence of defective ciliary Hh signaling. The fact that other signaling pathways, such as Wnt, BMP and PDGFR signaling, are crucial in cardiogenesis warrants further investigation on the signaling systems coordinated by the primary cilium, and whether these signaling systems impinge on ciliary Hh signaling in heart development.

Materials and Methods

Animals and tissue sectioning

Wild-type and Ift88-null (*Ift88*^{tm1Rpw}, *Ift88*$^{-/-}$) embryos were isolated from timed matings at E11.5. The Ift88-null embryos were generated from by intercrossing two *Ift88*^{tm1Rpw} heterozygotes congenic on the FVB/N genetic background. Tissue sectioning was performed as described (Nielsen et al., 2008). Serial sections, 3 to 5 μm thick, were cut sagittally and the amniotic sac was used for genotyping.

Cell culture

The P19.CL6 cell line is of mouse origin isolated from embryonal carcinoma tissue. The originator is Habara, Akemi and registered with Murofushi, Kimiko, Japan (ref. 2406 3467). The cells were grown in T75 cell culture flasks (Cellstar) at 37°C, 5% CO_2 and 95% humidity. Cells were cultured in MEM Alpha medium (Gibco), containing 1% penicillin-streptomycin (Gibco) and 10% foetal bovine serum (FBS, Gibco). The medium was supplemented with 1% dimethyl sulfoxide (DMSO, Merck) to induce cardiomyocyte differentiation. The cells were passaged every 2-3 days by trypsination (Trypsin-EDTA, Gibco). Swiss NIH3T3 mouse fibroblasts and primary cultures of embryonic fibroblasts (MEFs) from WT and ORPK (*Ifti88*^{Tg737RPW}, *Tg737*^{orpk}) mice were cultured as described (Schneider et al., 2005). Experimental cells were seeded at a confluency of about 30%.

Primary antibodies

Antibodies from Santa Cruz: rabbit anti-Gli3 (H-280) (Cat. no. SC-20688), goat anti-Gli2 (G-20) (SC-20291), goat anti-Gli3 (N-19) (SC-6155), goat anti-Gli2 (N-20) (SC-20290), goat anti-Gli3 (C-20) (SC-6154), rabbit anti-Gli2 (H-300) (SC-28674), goat anti-patched (G-19) (SC-6144), rabbit anti-Gata4 (H-112) (SC-9053), goat anti-Nkx-2,5 (N-19) (SC-8697); goat anti-Oct3/4 (C-20) (SC-8629); rabbit anti-Gli1 (Abcam AB14149); rabbit anti-Smo (MBL International LS2666); mouse anti-α-actinin (Sarcomeric) Sigma (A-7811); mouse anti-acetylated tubulin, Sigma (T7451); rabbit anti-detyrosinated α-tubulin (Glu-tubulin, Chemicon (AB3201); goat anti-Sox2 (R&D systems) (AF2018), mouse anti-Sox2 (R&D systems) (MAB2018). Secondary antibodies for immunofluorescence from Molecular Probes: Alexa Fluor® 568 Donkey IgG, anti-mouse (A10037), Alexa Fluor® 488 Donkey IgG, anti-goat (A11055), Alexa Fluor® 568 Donkey IgG, anti-rabbit (A21206). Secondary antibodies for western blot analysis: goat anti-mouse F(ab′)$_2$ specific alkaline phosphatase conjugated, Sigma (A1293), Goat anti-rabbit F(ab′)$_2$ specific alkaline phosphatase conjugated, Sigma (A3937), Rabbit anti-goat whole molecule alkaline phosphatase-conjugated, Sigma (A4187). DAPI: 4′,6-diamidino-2-phenylindole, dihydrochloride (Molecular Probes, D1306). Blocking peptides (BPs) (Santa Cruz): BP for goat anti-Gli2 (G-20) (SC-20291-P); BP for goat anti-Gli2 (N-20) (SC-20290-P).

siRNA constructs and transfection

The cells were transfected with the plasmids pGP678.12 and pJAF135.45 encoding siRNA targeted at mouse Ift88 and Ift20, respectively, by nucleofection with the Nucleofector device II from Amaxa Biosystems. We followed the recommended protocol for P19 cell transfection and used a Nucleofector Kit V. The recommended amount of cells for transfection was 2×10^6 and with 2 μg plasmid. Complementary oligonucleotides corresponding to the coding region of mouse Ift20 and mouse Ift88 were annealed and cloned into pGP676.13 digested with *Bgl*II and *Hin*dIII to produce pGP678.12 and pJAF135.45, respectively (Follit et al., 2006).

Immunofluorescence

The cells were grown on coverslips in six-well trays (TTP) and subjected to immunofluorescence microscopy analysis as described (Schneider et al., 2005). Pictures were captured with a cooled CCD Optronics camera on a Nikon-Japan, Eclipse E600 epifluorescence microscope and the digital images processed with Photoshop 6.0.

Histochemistry

Representative sections of WT and *Ift88*^{tm1Rpw} mice were stained with hematoxylin and eosin (H&E). In preparation for immunohistochemistry, tissue sections were heated for 1 hour at 60°C. Then, sections were deparaffinized for 10 minutes in xylene, 2 minutes in 99% ethanol, twice for 15 minutes in 99% ethanol, 15 minutes in 96% ethanol, 15 minutes in 70% ethanol and a final 15 minutes in H_2O. The sections were then placed in a tub with running tap water for 10 minutes and in PBS for 10 minutes. Sections were circled with a PAP pen and incubated in blocking buffer (PBS with 5% BSA) for 20 minutes. Immunohistochemistry was performed as described (Nielsen et al., 2008).

SDS-PAGE and western blot analysis

Cells were grown in Petri dishes and were rapidly washed once in PBS and spun down at 500 ***g*** for 5 minutes, after which 350 μl lysis buffer with 1% β-mercaptoethanol was added. Proteins were purified using Nucleospin kit protocol (Macherey-Nagel) for RNA or protein analysis. SDS-PAGE and western blotting were performed as described (Schneider et al., 2005).

Quantitative RT-PCR

RNA was purified using a Nucleospin kit (Macherey-Nagel). For cDNA synthesis we used DNase I Amplification grade (Invitrogen) and SuperScript™ II reverse transcriptase (Invitrogen). The Q-RT-PCR reactions were performed on a 7500 fast Realtime PCR-system from Applied Biosystems with Lightcycler Fast Start DNA Master plus SYBR Green 1 (Roche). Primers used are listed in supplementary material Table S1.

Statistics

We used one-way analysis of variance (ANOVA) test on n=3 or more. Significance levels were divided into three categories (*P<0.05, significant; **P<0.01, highly significant; ***P<0.001, extremely significant).

This work was supported by the Lundbeck Foundation, the Danish Science Research Council no. 272-07-0530 (S.T.C.), the Danish Heart Association (L.A.L.), funds from the Department of Biology, University of Copenhagen, Denmark (C.A.C.), by NIH RO1 HD056030 (B.K.Y.) and by GM60992 (G.J.P.). Wilhelm Johannsen Centre for Functional Genome Research is established by the Danish National Research Foundation. The authors would like to thank Lillian Rasmussen, Kirsten Winther, Venus Childress and Laura Smedegaard Kruuse for excellent technical assistance. Deposited in PMC for release after 12 months.

References

Angello, J. C., Kaestner, S., Welikson, R. E., Buskin, J. N. and Hauschka, S. D. (2007). BMP induction of cardiogenesis in P19 cells requires prior cell-cell interaction(s). *Dev. Dyn.* **235**, 2122-2133.

Awan, A., Oliveri, R. S., Jensen, P. L., Christensen, S. T. and Andersen, C. Y. (2009). Characterization of human embryonic stem cells (hESCs) grown under feeder-free conditions. *Methods in Molecular Biology* (ed. K. Turksen). Totowa, NJ: Humana Press.

Bellusci, S., Furuta, Y., Rush, M. G., Henderson, R., Winnier, G. and Hogan, B. L. (1997). Involvement of Sonic hedgehog (Shh) in mouse embryonic lung growth and morphogenesis. *Development* **124**, 53-63.

Breunig, J. J., Sarkisian, M. R., Arellano, J. I., Morozov, Y. M., Ayoub, A. E., Sojitra, S., Wang, B., Flavell, R. A., Rakic, P. and Town, T. (2008). Primary cilia regulate hippocampal neurogenesis by mediating sonic hedgehog signaling. *Proc. Natl. Acad. Sci. USA* **105**, 13127-13132.

Chen, J. K., Taipale, J., Young, K. E., Maiti, T. and Beachy, P. A. (2002). Small molecule modulation of Smoothened activity. *Proc. Natl. Acad. Sci. USA* **99**, 14071-14076.

Chizhikov, V. V., Davenport, J., Zhang, Q., Shih, E. K., Cabello, O. A., Fuchs, J. L., Yoder, B. K. and Millen, K. J. (2007). Cilia proteins control cerebellar morphogenesis by promoting expansion of the granule progenitor pool. *J. Neurosci.* **27**, 9780-9789.

Christensen, S. T. and Ott, C. M. (2007). Cell signaling: a ciliary signaling switch. *Science* **317**, 330-331.

Christensen, S. T., Pedersen, L. B., Schneider, L. and Satir, P. (2007) Sensory cilia and integration of signal transduction in human health and disease. *Traffic* **8**, 87-109.

Christensen, S. T., Pedersen, S. F., Satir, P., Veland, I. R. and Schneider, L. (2008). Chapter 10 the primary cilium coordinates signaling pathways in cell cycle control and migration during development and tissue repair. *Curr. Top. Dev. Biol.* **85**, 261-301.

Corbit, K. C., Aanstad, P., Singla, V., Norman, A. R., Stainier, D. Y. and Reiter, J. F. (2005). Vertebrate Smoothened functions at the primary cilium. *Nature* **437**, 1018-1021.

Corbit, K. C., Shyer, A. E., Dowdle, W. E., Gaulden, J., Singla, V., Chen, M. H., Chuang, P. T. and Reiter, J. F. (2008). Kif3a constrains beta-catenin-dependent Wnt signalling through dual ciliary and non-ciliary mechanisms. *Nat. Cell Biol.* **10**, 70-76.

Davenport, J. R. and Yoder, B. K. (2005). An incredible decade for the primary cilium: a look at a once-forgotten organelle. *Am. J. Physiol. Renal Physiol.* **289**, F1159-F1169.

Follit, J. A., Tuft, R. A., Fogarty, K. E. and Pazour, G. J. (2006). The intraflagellar transport protein Ift20 is associated with the golgi complex and is required for cilia assembly. *Mol. Biol. Cell* **17**, 3781-3792.

Follit, J. A., San Agustin, J. T., Xu, F., Jonassen, J. A., Samtani, R., Lo, C. W. and Pazour, G. J. (2008). The Golgin GMAP210/TRIP11 anchors Ift20 to the Golgi complex. *PLoS Genet.* **4**, e1000315.

Gerdes, J. M. and Katsanis, N. (2008). Chapter 7, Ciliary function and wnt signal modulation. *Curr. Top. Dev. Biol.* **85**, 175-195.

Gianakopoulos, P. J. and Skerjanc, I. S. (2005). Hedgehog signaling induces cardiomyogenesis in P19 cells. *J. Biol. Chem.* **280**, 21022-21028.

Goddeeris, M. M., Schwartz, R., Klingensmith, J. and Meyers, E. N. (2007). Independent requirements for Hedgehog signaling by both the anterior heart field and neural crest cells for outflow tract development. *Development* **134**, 1593-1604.

Gorivodsky, M., Mukhopadhyay, M., Wilsch-Braeuninger, M., Phillips, M., Teufel, A., Kim, C., Malik, N., Huttner, W. and Westphal, H. (2008). Intraflagellar transport protein 172 is essential for primary cilia formation and plays a vital role in patterning the mammalian brain. *Dev. Biol.* **325**, 24-32.

Grépin, C., Dagnino, L., Robitaille, L., Haberstroh, L., Antakly, T. and Nemer, M. (1994). A hormone-encoding gene identifies a pathway for cardiac but not skeletal muscle gene transcription. *Mol. Cell. Biol.* **14**, 3115-3129.

Grépin, C., Nemer, G. and Nemer, M. (1997). Enhanced cardiogenesis in embryonic stem cells overexpressing the GATA-4 transcription factor. *Development* **124**, 2387-2395.

Gouttenoire, J., Valcourt, U., Bougault, C., Aubert-Foucher, E., Arnaud, E., Giraud, L. and Mallein-Gerin, F. (2007). Knockdown of the intraflagellar transport protein Ift46 stimulates selective gene expression in mouse chondrocytes and affects early development in zebrafish. *J. Biol. Chem.* **282**, 30960-30973.

Habara-Ohkubo, A. (1996). Differentiation of beating cardiac muscle cells from a derivative of P19 embryonal carcinoma cells. *Cell Struct. Funct.* **21**, 101-110.

Han, Y. G., Spassky, N., Romanguera-Ros, M., Garcia-Verdugo, J. M., Aguilar, A., Schneider-Maunoury, S. and Alvarez-Buylla, A. (2008). Hedgehog signaling and primary cilia are required for the formation of adult neural stem cells. *Nat. Neurosci.* **11**, 277-284.

Haraguchi, K., Hayashi, T., Jimbo, T., Yamamoto, T. and Akiyama, T. (2006). Role of the kinesin-2 family protein, KIF3, during mitosis. *J. Biol. Chem.* **281**, 4094-4099.

Harris, P. C. and Torres, V. E. (2009). Polycystic kidney disease. *Annu. Rev. Med.* **60**, 321-327.

Haycraft, C. J., Swoboda, P., Taulman, P. D., Thomas, J. H. and Yoder, B. K. (2001). The C. elegans homolog of the murine cystic kidney disease gene Tg737 functions in a ciliogenic pathway and is disrupted in osm-5 mutant worms. *Development* **128**, 1493-1505.

Haycraft, C. J., Banizs, B., Aydin-Son, Y., Zhang, Q., Michaud, E. J. and Yoder, B. K. (2005). Gli2 and Gli3 localize to cilia and require the intraflagellar transport protein polaris for processing and function. *PLoS Genet.* **1**, e53.

Haycraft, C. J., Zhang, Q., Song, B., Jackson, W. S., Detloff, P. J., Serra, R. and Yoder, B. K. (2007). Intraflagellar transport is essential for endochondral bone formation. *Development* **134**, 307-316.

Hirata, H., Kawamata, S., Murakami, Y., Inoue, K., Nagahashi, A., Tosaka, M., Yoshimura, N., Miyamoto, Y., Iwasaki, H., Asahara, T. et al. (2007). Coexpression of platelet-derived growth factor receptor alpha and fetal liver kinase 1 enhances cardiogenic potential in embryonic stem cell differentiation in vitro. *J. Biosci. Bioeng.* **103**, 412-419.

Huangfu, D. and Anderson, K. V. (2005). Cilia and Hedgehog responsiveness in the mouse. *Proc. Natl. Acad. Sci. USA* **102**, 11325-11330.

Huangfu, D. and Anderson, K. V. (2006). Signaling from Smo to Ci/Gli: conservation and divergence of Hedgehog pathways from Drosophila to vertebrates. *Development* **133**, 3-14.

Hynes, M., Stone, D. M., Dowd, M., Pitts-Meek, S., Goddard, A., Gurney, A. and Rosenthal, A. (1997). Control of cell pattern in the neural tube by the zinc finger transcription factor and oncogene Gli-1. *Neuron* **19**, 15-26.

Iomini, C., Tejada, K., Mo, W., Vaananen, H. and Piperno, G. (2004). Primary cilia of human endothelial cells disassemble under laminar shear stress. *J. Cell Biol.* **164**, 811-817.

Johnson, E. T., Nicola, T., Roarty, K., Yoder, B. K., Haycraft, C. J. and Serra, R. (2008). Role for primary cilia in the regulation of mouse ovarian function. *Dev. Dyn.* **237**, 2053-2060.

Johnson, R. L., Riddle, R. D., Laufer, E. and Tabin, C. (1994). Sonic hedgehog: a key mediator of anterior-posterior patterning of the limb and dorso-ventral patterning of axial embryonic structures. *Biochem. Soc. Trans.* **22**, 569-574.

Kiprilov, E. N., Awan, A., Desprat, R., Velho, M., Clement, C. A., Byskov, A. G., Andersen, C. Y., Satir, P., Bouhassira, E. E., Christensen, S. T. et al. (2008). Human embryonic stem cells in culture possess primary cilia with hedgehog signaling machinery. *J. Cell Biol.* **180**, 897-904.

Kuo, C. T., Morrisey, E. E., Anandappa, R., Sigrist, K., Lu, M. M., Parmacek, M. S., Soudais, C. and Leiden, J. M. (1997). GATA4 transcription factor is required for ventral morphogenesis and heart tube formation. *Genes Dev.* **11**, 1048-1060.

Kwon, C., Cordes, K. R. and Srivastava, D. (2008). Wnt/beta-catenin signaling acts at multiple developmental stages to promote mammalian cardiogenesis. *Cell Cycle* **7**, 3815-3818.

Lavine, K. J., Kovacs, A. and Ornitz, D. M. (2008). Hedgehog signaling is critical for maintenance of the adult coronary vasculature in mice. *J. Clin Invest.* **118**, 2404-2414.

Lehman, J. M., Michaud, E. J., Schoeb, T. R., Aydin-Son, Y., Miller, M. and Yoder, B. K. (2008). The Oak Ridge Polycystic Kidney mouse: modeling ciliopathies of mice and men. *Dev. Dyn.* 1960-1971.

Lints, T. J., Parsons, L. M., Hartley, L., Lyons, I. and Harvey, R. P. (1993). *Nkx2-5*: a novel murine homeobox gene expressed in early heart progenitor cells and their myogenic descendants. *Development* **119**, 419-431.

Liu, A., Wang, B. and Niswander, L. A. (2005). Mouse intraflagellar transport proteins regulate both the activator and repressor functions of Gli transcription factors. *Development* **132**, 3103-3111.

Lucker, B. F., Behal, R. H., Qin, H., Siron, L. C., Taggart, W. D., Rosenbaum, J. L. and Cole, D. G. (2005). Characterization of the intraflagellar transport complex B core: direct interaction of the Ift81 and Ift74/72 subunits. *J. Biol. Chem.* **280**, 27688-27696.

Lyons, G. E. (1994). In situ analysis of the cardiac muscle gene program during embryogenesis. Trends. *Cardiovasc. Med.* **4**, 70-77.

Masui, S., Nakatake, Y., Toyooka, Y., Shimosato, D., Yagi, R., Takahashi, K., Okochi, H., Okuda, A., Matoba, R., Sharov, A. A. et al. (2007). Pluripotency governed by Sox2 via regulation of Oct3/4 expression in mouse embryonic stem cells. *Nat. Cell Biol.* **9**, 625-635.

May, S. R., Ashique, A. M., Karlen, M., Wang, B., Shen, Y., Zarbalis, K., Reiter, J., Ericson, J. and Peterson, A. S. (2005). Loss of the retrograde motor for IFT disrupts localization of Smo to cilia and prevents the expression of both activator and repressor functions of Gli. *Dev. Biol.* **287**, 378-389.

Moyer, J. H., Lee-Tischler, M. J., Kwon, H. Y., Schrick, J. J., Avner, E. D., Sweeney, W. E., Godfrey, V. L., Cacheiro, N. L., Wilkinson, J. E. and Woychik, R. P. (1994). Candidate gene associated with a mutation causing recessive polycystic kidney disease in mice. *Science* **264**, 1329-1333.

Murcia, N. S., Richards, W. G., Yoder, B. K., Mucenski, M. L., Dunlap, J. R. and Woychik, R. P. (2000). The Oak Ridge Polycystic Kidney (orpk) disease gene is required for left-right axis determination. *Development* **127**, 2347-2355.

Nauli, S. M., Kawanabe, Y., Kaminski, J. J., Pearce, W. J., Ingber, D. E. and Zhou, J. (2008). Endothelial cilia are fluid shear sensors that regulate calcium signaling and nitric oxide production through polycystin-1. *Circulation* **117**, 1161-1171.

Nielsen, S. K., Møllgård, K., Clement, C. A., Veland, I. R., Awan, A., Yoder, B. K., Novak, I. and Christensen, S. T. (2008). Characterization of primary cilia and Hedgehog signaling during development of the human pancreas and in human pancreatic duct cancer cell lines. *Dev. Dyn.* **237**, 2039-2052.

Nonaka, S., Tanaka, Y., Okada, Y., Takeda, S., Harada, A., Kanai, Y., Kido, M. and Hirokawa, N. (1998). Randomization of left-right asymmetry due to loss of nodal cilia generating leftward flow of extraembryonic fluid in mice lacking KIF3B motor protein. *Cell* **95**, 829-837.

Ocbina, P. J. and Anderson, K. V. (2008). Intraflagellar transport, cilia, and mammalian Hedgehog signaling: analysis in mouse embryonic fibroblasts. *Dev. Dyn.* **237**, 2030-2038.

Pan, J. (2008). Cilia and ciliopathies: from Chlamydomonas and beyond. *Sci. China C Life Sci.* **51**, 479-486.

Pan, Y., Bai, C. B., Joyner, A. L. and Wang, B. (2006). Sonic hedgehog signaling regulates Gli2 transcriptional activity by suppressing its processing and degradation. *Mol. Cell. Biol.* **26**, 3365-3377.

Paquin, J., Danalache, B. A., Jankowski, M., McCann, S. M. and Gutkowska, J. (2002). Oxytocin induces differentiation of P19 embryonic stem cells to cardiomyocytes. *Proc. Natl. Acad. Sci. USA* **99**, 9550-9555.

Pazour, G. J., Dickert, B. L., Vucica, Y., Seeley, E. S., Rosenbaum, J. L., Witman, G. B. and Cole, D. G. (2000). Chlamydomonas Ift88 and its mouse homologue, polycystic kidney disease gene tg737, are required for assembly of cilia and flagella. *J. Cell Biol.* **151**, 709-718.

Pedersen, L. B., Veland, I. R., Schrøder, J. M. and Christensen, S. T. (2008). Assembly of primary cilia. *Dev. Dyn.* **237**, 1993-2006.

Pesce, M. and Scholer, H. R. (2001). Oct-4: gatekeeper in the beginnings of mammalian development. *Stem Cells* **19**, 271-278.

Rohatgi, R., Milenkovic, L. and Scott, M. P. (2007). Patched1 regulates hedgehog signaling at the primary cilium. *Science* **317**, 372-376.

Rosenbaum, J. L. and Witman, G. B. (2002). Intraflagellar transport. *Nat. Rev. Mol. Cell. Biol.* **3**, 813-825.

Ruiz I Altaba, A. (1999). Gli proteins encode context-dependent positive and negative functions: implications for development and disease. *Development* **126**, 3205-3216.

Satir, P. and Christensen, S. T. (2007). Overview of structure and function of mammalian cilia. *Annu. Rev. Physiol.* **69**, 377-400.

Schneider, L., Clement, C. A., Teilmann, S. C., Pazour, G. J., Hoffmann, E. K., Satir, P. and Christensen, S. T. (2005). PDGFRaa signaling is regulated through the primary cilium in fibroblasts. *Curr. Biol.* **15**, 1861-1866.

Skerjanc, I. S. (1999). Cardiac and skeletal muscle development in P19 embryonal carcinoma cells. *Trends Cardiovasc. Med.* **9**, 139-143.

Slough, J., Cooney, L. and Brueckner, M. (2008). Monocilia in the embryonic mouse heart suggest a direct role for cilia in cardiac morphogenesis. *Dev. Dyn.* **237**, 2304-2314.

Journal of Cell Science

Spassky, N., Han, Y. G., Aguilar, A., Strehl, L., Besse, L., Laclef, C., Ros, M. R., Garcia-Verdugo, J. M. and Alvarez-Buylla, A. (2008). Primary cilia are required for cerebellar development and Shh-dependent expansion of progenitor pool. *Dev. Biol.* **317**, 246-259.

Sucov, H. M. (1998). Molecular insights into cardiac development. *Annu. Rev. Physiol.* **60**, 287-308.

Takeda, S., Yonekawa, Y., Tanaka, Y., Okada, Y., Nonaka, S. and Hirokawa, N. (1999). Left-right asymmetry and kinesin superfamily protein KIF3A: new insights in determination of laterality and mesoderm induction by kif3A$^{-/-}$ mice analysis. *J. Cell Biol.* **145**, 825-836.

Takei, S., Ichikawa, H., Johkura, K., Mogi, A., No, H., Yoshie, S., Tomotsune, D. and Sasaki, K. (2009). Bone morphogenetic protein-4 promotes induction of cardiomyocytes from human embryonic stem cells in serum-based embryoid body development. *Am. J. Physiol. Heart Circ. Physiol.* **296**, H1793-H1803.

Taulman, P. D., Haycraft, C. J., Balkovetz, D. F. and Yoder, B. K. (2001). Polaris, a protein involved in left-right axis patterning, localizes to basal bodies and cilia. *Mol. Biol. Cell* **12**, 589-599.

Teng, J., Rai, T., Tanaka, Y., Takei, Y., Nakata, T., Hirasawa, M., Kulkarni, A. B. and Hirokawa, N. (2005). The KIF3 motor transports N-cadherin and organizes the developing neuroepithelium. *Nat. Cell Biol.* **7**, 474-482.

Tsukui, T., Capdevila, J., Tamura, K., Ruiz-Lozano, P., Rodriguez-Esteban, C., Yonei-Tamura, S., Magallón, J., Chandraratna, R. A., Chien, K., Blumberg, B. et al. (1999). Multiple left-right asymmetry defects in Shh(–/–) mutant mice unveil a convergence of the shh and retinoic acid pathways in the control of Lefty-1. *Proc. Natl. Acad. Sci. USA* **96**, 11376-11381.

Uchida, S., Fuke, S. and Tsukahara, T. (2007). Upregulations of Gata4 and oxytocin receptor are important in cardiomyocyte differentiation processes of P19CL6 cells. *J. Cell Biochem.* **100**, 629-641.

van Wijk, B., Moorman, A. F. and van den Hoff, M. J. (2007). Role of bone morphogenetic proteins in cardiac differentiation. *Cardiovasc. Res.* **74**, 244-255.

Washington Smoak, I., Byrd, N. A., Abu-Issa, R., Goddeeris, M. M., Anderson, R., Morris, J., Yamamura, K., Klingensmith, J. and Meyers, E. N. (2005). Sonic hedgehog is required for cardiac outflow tract and neural crest cell development. *Dev. Biol.* **283**, 357-372.

Wong, S. Y. and Reiter, J. F. (2008). Chapter 9 the primary cilium at the crossroads of Mammalian hedgehog signaling. *Curr. Top. Dev. Biol.* **85**, 225-260.

Yamazaki, H., Nakata, T., Okada, Y. and Hirokawa, N. (1995). KIF3A/B: a heterodimeric kinesin superfamily protein that works as a microtubule plus end-directed motor for membrane organelle transport. *J. Cell Biol.* **130**, 1387-1399.

Yoder, B. K., Tousson, A., Millican, L., Wu, J. H., Bugg, C. E., Jr, Schafer, J. A. and Balkovetz, D. F. (2002). Polaris, a protein disrupted in orpk mutant mice, is required for assembly of renal cilium. *Am. J. Physiol. Renal Physiol.* **282**, F541-F552.

Zhang, X. M., Ramalho-Santos, M. and McMahon, A. P. (2001). Smoothened mutants reveal redundant roles for Shh and Ihh signaling including regulation of L/R symmetry by the mouse node. *Cell* **106**, 781-792.